Journal of Power Sources 254 (2014) 293–297

Contents lists available at ScienceDirect

Journal of Power Sources

journal homepage: www.elsevier.com/locate/jpowsour

Short communication

# Charge transfer in Li/$CF_x$–silver vanadium oxide hybrid cathode batteries revealed by solid state $^{7}Li$ and $^{19}F$ nuclear magnetic resonance spectroscopy

Paul J. Sideris [a,1], Rowena Yew [a], Ian Nieves [a], Kaimin Chen [b], Gaurav Jain [b], Craig L. Schmidt [b], Steve G. Greenbaum [a,*]

[a] Department of Physics and Astronomy, Hunter College of CUNY, New York, NY 10065, USA
[b] Medtronic Energy and Component Center, Brooklyn Center, MN 55430, USA

## HIGHLIGHTS

- Hybrid cathodes containing $CF_x$ and silver vanadium oxide were investigated using NMR.
- $^{7}Li$ and $^{19}F$ NMR signals were compared for samples after various periods of rest.
- After 1 and 3 months of rest, the relative amount of LiF in the cells increased.
- Changes in peak intensities are attributed to $Li^{+}$ migration between the two phases.

## ARTICLE INFO

*Article history:*
Received 23 November 2013
Received in revised form
24 December 2013
Accepted 26 December 2013
Available online 4 January 2014

*Keywords:*
Lithium batteries
Hybrid cathode
NMR
$CF_x$
$Ag_2V_4O_{11}$

## ABSTRACT

Solid state $^{7}Li$ and $^{19}F$ magic angle spinning nuclear magnetic resonance (MAS NMR) experiments are conducted on several cathodes containing $CF_x$–Silver vanadium oxide ($CF_x$–$Ag_2V_4O_{11}$) hybrid cathodes discharged to 50% depth of discharge (DoD) and stored at their open-circuit voltage for a period of one and three months. Three carbonaceous sources for the $CF_x$ phase are investigated: petroleum coke-based, fibrous, and mixed fibrous. For each hybrid cathode, a measurable increase in the relative amount of lithium fluoride is observed after a three month resting period in both the $^{7}Li$ and $^{19}F$ NMR spectra. These changes are attributed to lithium ion migration from the silver vanadium oxide to the $CF_x$ phase during the resting period, and help clarify the mechanism behind high power handling capability of this cathode.

© 2014 Elsevier B.V. All rights reserved.

## 1. Introduction

Modern pacemakers and other implantable medical devices, such as neurostimulators and drug delivery pumps, have unique power requirements that have spearheaded innovations in lithium battery technology. General requirements for the batteries in these devices include safety, reliability, high energy density, a small footprint, low self-discharge (which are capacity losses due to chemical side-reactions in the cell), and predictable end-of-life indicators in the discharge profile. Among the unique power requirements of implantable cardiac defibrillators (ICDs), for example, are continuous microampere current drain over the life-span of the device (typically several years), as well as the ability to rapidly deploy high current pulses on the order of a few amperes if fibrillation is detected. Advances such as multi-site pacing, programmability, and telemetric functionality of these devices further necessitates power sources with high energy densities and flexible rate capability [1,2]. To meet these needs, Li/$CF_x$ and Li/$Ag_2V_4O_{11}$ (Li/SVO) cells were developed [3–5].

$CF_x$, where $x$ is nominally 1.0 for commercial grade products, is synthesized by reacting $F_2$ gas with carbon at elevated temperatures up to approximately 600 °C. The theoretical gravimetric capacity of $CF_x$ is 864 mAh $g^{-1}$. Li/$CF_x$ cells also have a relatively high voltage of 3.0 V, Fig. 1a. The chemical reactions in the discharge process of $CF_x$ can be written as:

* Corresponding author. Tel.: +1 212 772 4973; fax: +1 212 772 5390.
*E-mail address:* steve.greenbaum@hunter.cuny.edu (S.G. Greenbaum).
[1] Present address: Department of Chemistry, CUNY Queensborough Community College, Bayside, NY 11364, USA.

0378-7753/$ – see front matter © 2014 Elsevier B.V. All rights reserved.
http://dx.doi.org/10.1016/j.jpowsour.2013.12.108

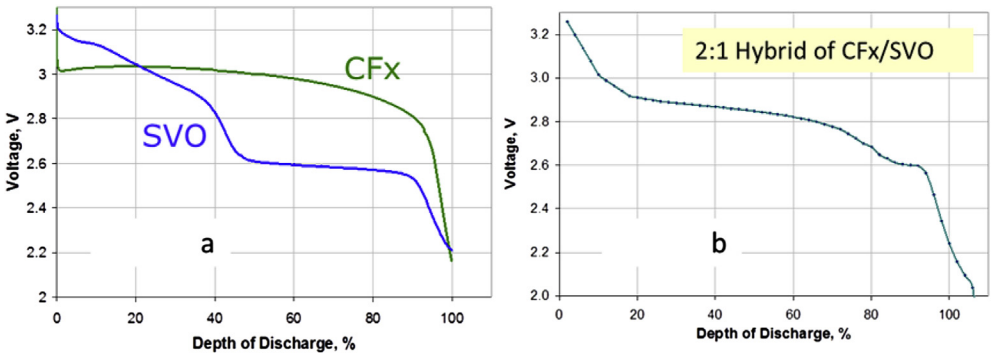


**Fig. 1.** Plots of cell voltage vs. depth of discharge. a) Li/$CF_x$ and Li/SVO; b) Li/$CF_x$–SVO hybrid. The carbon source of the $CF_x$ in this graph was petroleum coke.

Anode: $x\mathrm{Li} \rightarrow x\mathrm{Li}^{+} + x\mathrm{e}^{-}$

Cathode: $x\mathrm{e}^{-} + \mathrm{CF}_x \rightarrow \mathrm{C} + x\mathrm{F}^{-}$

Overall reaction: $x\mathrm{Li} + \mathrm{CF}_x \rightarrow x\mathrm{LiF} + \mathrm{C}$

During lithiation, elemental carbon and lithium fluoride are formed. [6–8] The elemental carbon is more conductive than the pristine $CF_x$ material, which lowers the internal impedance of the cell and improves the efficiency.

Since the mid-1980s, Li/SVO batteries have been incorporated into the majority of ICDs, where high currents are required for operation. [9] The theoretical gravimetric capacity of SVO is 315 mAh $g^{-1}$. The overall cell reaction is given by:

$7\mathrm{Li} + \mathrm{Ag_2V_4O_{11}} \rightarrow \mathrm{Li_7Ag_2V_4O_{11}}$

During the early stages of lithiation of $\mathrm{Li}_x\mathrm{Ag_2V_4O_{11}}$ ($0 < x < 2.4$), a loss of crystallinity is observed as $Ag^{+}$ gets reduced to nano-sized metallic $Ag^{0}$. The formation and extrusion of metallic silver from SVO greatly increases the conductivity of the cathode and contributes to the high current-carrying property of the system. For $x > 2.4$, reduction of $V^{5+}$ to $V^{4+}$ and $V^{3+}$ occurs resulting in formation of mixed-valence materials [10–19].

Another attractive property of the Li/SVO battery is a stepped voltage–capacity curve with a plateau near the end of the discharge due to the presence of many oxidation states of vanadium and the reduction of silver, Fig. 1a. This end-of-life plateau serves as a reliable warning prior to the depletion of the battery [10,13–15]. In contrast, the Li/$CF_x$ battery has a higher energy density, but due to a voltage-curve that is mostly flat during discharge before a steep decline, does not have an ample end-of-service warning [3].

Recently, Medtronic introduced a hybrid cathode composed of mixtures of $CF_x$ and SVO which displays the desirable properties of high energy density and high rate capability. The energy density is comparable to that of traditional Li/$I_2$ batteries, but with two orders of magnitude higher power density. [3] Additionally, the hybrid cathode exhibits the same end-of-service warning in the discharge profile as the Li/SVO battery, as shown in Fig. 1b, in which the carbon source for the $CF_x$ was petroleum coke (which will be discussed later). Altering the $CF_x$ and SVO ratio of the hybrid cathode, coupled with choice of the electrolyte, allows for the power-energy characteristics as well as the time between the end-of-service warning and the depletion of the battery to be tuned for desired performance profiles. As such, it is desirable to understand the electrochemical interactions between $CF_x$ and SVO in different states of discharge. Conventional belief is that during high power demands, majority of capacity is delivered by discharge of the SVO and upon rest the SVO is recharged while CFx is gradually discharged. The amount of CFx discharge during the high power event and the subsequent recharge of SVO varies with the CFx type. At present, there have been no reports on the mechanism of charge transfer between the two phases, nor details regarding the kinetics of the process. The goal of this paper is to apply NMR to provide evidence of this process at the atomic level.

Here, $^{7}$Li and $^{19}$F MAS NMR measurements of various $CF_x$/SVO hybrid cathodes, where different carbonaceous sources of the $CF_x$ were used (petroleum coke-based, fibrous, and mixed fibrous), are presented which demonstrate, in each case, a small increase in the relative amount of lithium fluoride as a function of resting time for a given depth of discharge. This change is attributed to charge transfer that occurs via physical contact between cathode particles during rest whereby lithium ions initially inserted into the SVO phase transfer to the $CF_x$ phase to form LiF. These effects are observable despite a relatively low current density (125 μA $cm^{-2}$) during discharge. To our knowledge, this is the first demonstration of charge transfer at the atomic or molecular level.

## 2. Experimental

Hybrid cathodes were prepared by mixing $CF_x$ and $\mathrm{Ag_2V_4O_{11}}$ in a 2:1 ratio by capacity. The electrolyte for each cell was 1 M $LiAsF_6$ dissolved in a 1:1 mixture by volume of propylene carbonate (PC) and dimethoxyethane (DME). Carbon black was added to make the cathodes more conductive. Each cell contained a binder composed of polytetrafluoroethylene (PTFE). Cells were electrochemically discharged at 125 μA $cm^{-2}$ to the target depth of discharge at 37 °C. One set of cells were disassembled immediately after discharge and the remaining cells were then left at ambient temperature at their open circuit voltage for a period of either 1 month or 3 months. The cathodes were recovered and washed with the PC/DME mixture first and then with pure DME. The cathode materials were dried under vacuum at approximately 90 °C.

Solid state $^{19}$F and $^{7}$Li magic angle spinning nuclear magnetic resonance spectroscopy was performed at 7 T using a Varian S Direct Digital Drive spectrometer operating at 283.27 and 117.13 MHz respectively. All the experiments were performed on a Varian 1.6 mm FastMAS double-resonance probe. Samples were packed in 1.6 mm rotors inside an argon glove box and spun to approximately 30 kHz using compressed air. In order to minimize background fluorine signal from the fluoroplastic components in the probe and to flatten the baseline of the spectra, a Hahn echo pulse sequence was used for the $^{19}$F NMR measurements. A radiofrequency field strength of approximately 140 kHz was used for each echo experiment. A single rotor period (33.33 μs) was employed between the 90° and 180° radiofrequency pulses. The recycle delay was between 100 and 240 s, depending on the

sample, to ensure quantitative results. $^{7}$Li data were collected using direct excitation, with a radiofrequency field strength of approximately 160 kHz. The recycle delays were between 80 and 120 s. An aqueous solution of lithium triflate was used as a secondary reference for both $^{19}$F (−78.5 ppm relative to the standard $CFCl_3$) and $^{7}$Li (0 ppm relative to the standard $LiCl_{(aq)}$). NMR data were processed using the WinNuts software package. The free induction decay was apodized using a single exponential (LB = 50 Hz) before Fourier transformation.

## 3. Results and discussion

Fig. 2 shows representative $^{19}$F spectra of the hybrid cathodes as a function of depth of discharge (DoD) without any rest period, along with a $CF_x$ reference spectrum. The spectra have chemical shifts and breadths that are consistent with those expected from previously studied fluorinated carbonaceous materials. [17,20–25] The pristine $CF_x$ material has isotropic resonances at approximately −185, −170, −120, and −113 ppm. The majority of the fluorine intensity for each $CF_x$ sample arises from the peaks at −185 and −170 ppm. The resonance at −185 ppm is the most intense and narrow. The peak centered about −170 ppm is partially resolved and appears as a broad shoulder. The peaks at −125 and −113 ppm have relatively smaller amplitudes to the other two sites and have comparable intensity. The $^{19}$F MAS NMR spectra of cathodes harvested from discharged batteries contain three additional resonances: a very intense peak at −207 ppm, a narrow resonance at −123 ppm with a large amplitude, and a weak peak at −70 ppm. On the basis of chemical shift, these peaks are assigned to fluorine in LiF, the binder, and residual $AsF_6^-$ from the electrolyte, respectively. [22,23] As the battery is discharged, the LiF component increases in intensity while all of the resonances of the $CF_x$ decrease in intensity. By 80% DoD, the $^{19}$F spectra are dominated by the LiF signal. The remaining intensity of the resonances from the $CF_x$ material are greatly reduced to the point where they appear as broad features in the baseline. These spectral features are consistent with the proposed mechanism of lithiation during discharge.

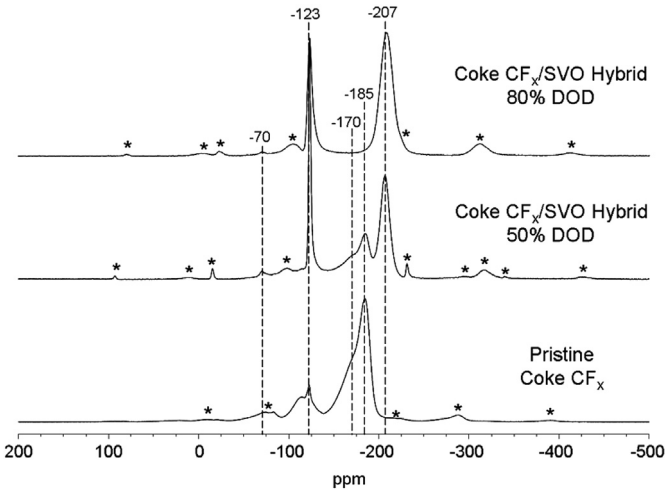


**Fig. 2.** Representative $^{19}$F MAS NMR spectra of $CF_x$/SVO hybrid cathodes as a function of depth of discharge and 0 rest time. Cathode materials from petroleum coke-based $CF_x$ are shown. The pristine $CF_x$ samples have isotropic shifts at approximately −113, −120, −170, and −185 ppm. A sharp, intense binder peak is present at −123 ppm. During discharge, a resonance at −207 ppm appears, indicative of LiF. A weak resonance at −70 ppm is attributed to residual electrolyte salt, $LiAsF_6$. Asterisks denote spinning sidebands.

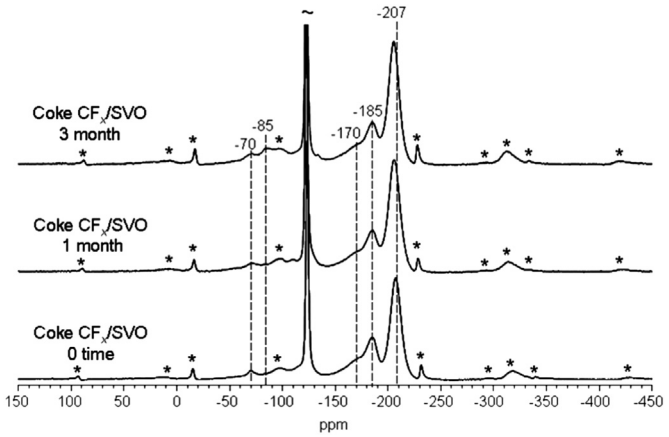


**Fig. 3.** Stack plot of the $^{19}$F MAS NMR spectra of the Coke $CF_x$/SVO hybrid cathode as a function of resting period. Isotropic resonances and spinning sidebands are denoted by dashed lines and asterisks respectively. A resonance at approximately −85 ppm, tentatively assigned to an electrolyte decomposition product, appears after a 1 month resting period and increases in intensity between 1 and 3 months of rest. The sharp resonance at approximately −123 ppm is due to the binder.

In order to more accurately quantify any site-specific changes in the $^{19}$F NMR intensity due to charge transfer, a 50% DoD was targeted for cells that with rest periods of 1 and 3 months. Fig. 3 shows the $^{19}$F MAS NMR spectra of a representative sample, the Coke $CF_x$/SVO hybrid cathode, discharged to 50% DoD as a function of resting time. A new resonance at approximately −85 ppm appears after 1 month rest and increases in intensity by 3 months. This resonance

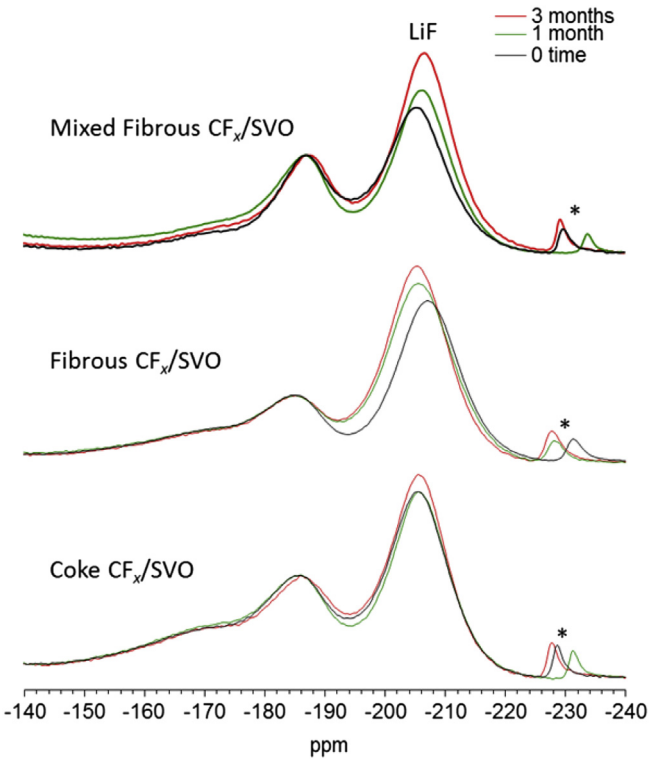


**Fig. 4.** $^{19}$F MAS NMR spectra of the various $CF_x$/SVO hybrid cathodes discharged to 50% DoD as a function of resting time – 3 months (red), 1 month (green), 0 time (black). A spinning sideband of the binder peak (isotropic resonance not shown) is marked by an asterisk. Very slight differences in sample spinning speed resulted in sidebands that do not overlap exactly. The spectra are normalized with respect to the peak at −185 ppm. The peak due to LiF appears at approximately −207 ppm.

is tentatively assigned to an electrolyte decomposition product. The mechanism for such decomposition on the cathode side is not known, but it is possible that such products forming on the anode side could migrate through the electrolyte and wind up in the cathode.

Fig. 4 displays the $^{19}$F MAS NMR spectra of all the $CF_x$/SVO hybrid cathodes discharged to 50% DoD as a function of resting period. The overlaid spectra were normalized with respect to the resonance at −185 ppm at 0 time for each sample and displayed from −140 to −240 ppm to emphasize the changes in intensity of the main spectroscopic features. For each hybrid cathode, there is a slight increase in the intensity of the LiF resonance by the 3 month resting period. The fibrous and mixed fibrous $CF_x$ samples both show a slight increase in the intensity of the LiF resonance during 1 month rest.

These relative changes in intensity of the LiF peak during the resting periods are attributed to $Li^+$ transfer from the SVO phase to the $CF_x$ phase. The resonances at approximately −170 and −185 ppm are overlaid on top of each other in the normalized plots of the Coke and Fibrous $CF_x$/SVO cathodes, implying that the source of fluorine to produce the LiF during the $Li^+$ transfer from the SVO to the $CF_x$ phase arises from both of these chemical environments.

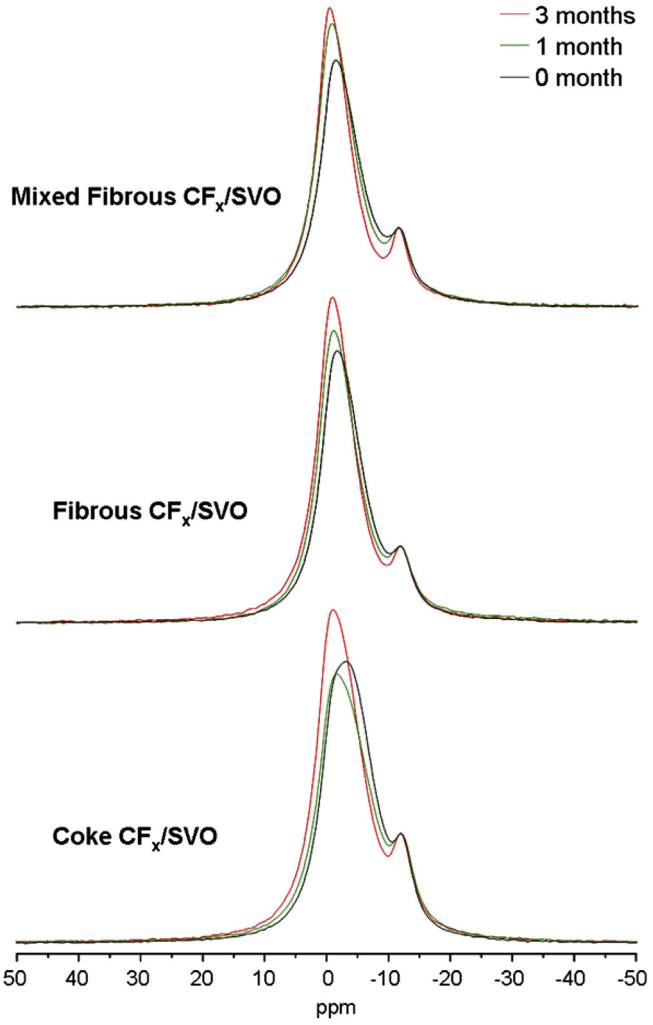


**Fig. 5.** $^7$Li MAS NMR spectra of each $CF_x$/SVO hybrid cathode discharged to 50% DoD as a function of resting period – 3 months (red), 1 month (green), 0 time (black). Only the isotropic region is displayed. Two resonances are resolved at approximately 0 and −12 ppm. All spectra are normalized to the peak at −12 ppm.

**Table 1**
Percent changes in the amount of LiF present in the coke, fibrous, and mixed fibrous $CF_x$/SVO hybrid cathodes discharged to 50% DoD after a resting period of 1 and 3 months, relative to 0 time. The intensities of the isotropic LiF peaks (approximately −207 ppm for the $^{19}$F) were used in the analysis.

| Relative percent change (%) in LiF from the $^7$Li and $^{19}$F MAS NMR data with resting period | | |
|---|---|---|
| Sample | 1 month | 3 month |
| Coke $CF_x$/SVO | 10 | 13 |
| Fibrous $CF_x$/SVO | 0 | 8 |
| Mixed Fibrous $CF_x$/SVO | 10 | 20 |

Fig. 5 shows the $^7$Li MAS NMR spectra of the hybrid cathodes discharged to a DoD of 50% as a function of resting period. Two resonances can be resolved, centered at approximately 0 and −12 ppm. All spectra are normalized with respect to the −12 ppm peak. The resonance at 0 ppm is much more intense and broad relative to the one at −12 ppm. Diamagnetic lithium environments, such as those present in the electrolyte salt ($LiAsF_6$), solid electrolyte interphase (SEI), and lithium fluoride, all resonate at approximately 0 ppm [26]. This intense peak contains contributions from each of these environments. There are slight differences in the line width of this resonance in the samples that are attributed to corresponding variations of the above components.

Based on the relative intensities of the LiF and residual $LiAsF_6$ environments, as determined by the $^{19}$F MAS NMR spectra, the lithium signal around 0 ppm is dominated by the LiF contribution. The resonance at −12 ppm is assigned to lithium intercalated into SVO during the initial stages of discharge, where $Li^+$ replaces $Ag^+$ in the structure, as reported previously [17]. The presence of the −12 ppm peak in the $^7$Li spectra and the −207 ppm (LiF) peak in the $^{19}$F spectra of each sample confirms the insertion of lithium into both the SVO and $CF_x$ phases during discharge. The relatively weaker intensity of the −12 ppm peak can be attributed to the following: (i) the hybrid cathodes contained more $CF_x$ than SVO (2:1), and (ii) the cells were discharged at a relatively low current density (125 μA cm$^{-2}$), which permits comparable lithium insertion into both the SVO and $CF_x$ phases. Both factors increase the production of LiF and consequently the intensity at approximately 0 ppm.

By 3 months of rest at the OCV, the relative intensity of the 0 ppm peak increases for each sample. Another factor in the increase of the 0 ppm relative to −12 ppm component is the decrease of Li in the SVO phase (again, the spectra are normalized with respect to the −12 ppm peak at zero time). Moreover, the center of gravity of the lithium signal shifts closer toward 0 ppm. These results are consistent with the $^{19}$F NMR data which featured an increase in the amount of LiF that occurs via $Li^+$ transfer from the SVO to $CF_x$ phase. Attempts to quantify the changes in intensity for $^{19}$F MAS NMR data are presented in Table 1. The data are presented as a percent change in the LiF environment (−207 ppm peak) relative to the 0 time sample. A 3% error in the relative percentages was estimated by performing the spectral deconvolutions and integrations multiple times.

## 4. Conclusions

Multinuclear MAS NMR studies were performed on discharged $CF_x$–SVO hybrid cathodes. Characteristic signals arising from the insertion of lithium ions into both the $CF_x$ and SVO phases were observed. Additionally, $^7$Li and $^{19}$F data have shown a measurable change in the relative intensity of lithium fluoride during a resting time of 3 months after achieving a target depth of discharge (50%) at a modest current density of 125 μA cm$^{-2}$. This change is

attributed to lithium-ion transfer from the SVO to the $CF_x$ phase, during rest, thereby producing LiF. The result provides direct evidence of the charge transfer between SVO and $CF_x$ in this binary active cathode system. Understanding of the charge transfer kinetics could lead to further optimization of the SVO/$CF_x$ hybrid for applications with diverse power requirements.

## Acknowledgments

The battery materials NMR program at Hunter College is funded by the Department of Energy, Division of Basic Energy Sciences, Grant no. DE-SC0005029. I.N. thanks the Hunter College Center for Gene Structure and Function, funded by the National Institutes of Health (RR 003037) for Fellowship Support. P.J.S and S.G.G. thank the City University of New York Collaborative Incentive Research Grant (CUNY CIRG) Round 20 for financial support.

## References

[1] C.F. Holmes, J. Power Sources 97–98 (2001) 739–741.
[2] C.L. Schmidt, P.M. Skarstad, J. Power Sources 97–98 (2001) 742–746.
[3] K. Chen, D.R. Merritt, W.G. Howard, C.L. Schmidt, P.M. Skarstad, J. Power Sources 162 (2006) 837–840.
[4] H. Gan, R.S. Rubino, E.S. Takeuchi, J. Power Sources 146 (2005) 101–106.
[5] P. Meduri, H. Chen, X. Chen, J. Xiao, M.E. Gross, T.J. Carlson, J.-G. Zhang, D. Deng, Electrochem. Commun. 13 (2011) 1344–1348.
[6] N. Watanabe, M. Endo, K. Ueno, Solid State Ionics 1 (1980) 501–507.
[7] N. Watanabe, Phys. B+C 105 (1981) 17–21.
[8] H. Touhara, H. Fujimoto, N. Watanabe, A. Tressaud, Solid State Ionics 14 (1984) 163–170.
[9] K.J. Takeuchi, A.C. Marschilok, S.M. Davis, R.A. Leising, E.S. Takeuchi, Coord. Chem. Rev. 219–221 (2001) 283–310.
[10] E.S. Takeuchi, W.C. Thiebolt III, J. Electrochem. Soc. 135 (1988) 2691–2694.
[11] F. Garcia-Alvarado, J.M. Tarascon, Solid State Ionics 73 (1994) 247–254.
[12] R.A. Leising, W.C. Thiebolt III, E.S. Takeuchi, Inorg. Chem. 33 (1994) 5733–5740.
[13] A.M. Crespi, P.M. Skarstad, H.W. Zandbergen, J. Power Sources 54 (1995) 68–71.
[14] K. West, A.M. Crespi, J. Power Sources 54 (1995) 334–337.
[15] A. Crespi, C. Schmidt, J. Norton, K. Chen, P. Skarstad, J. Electrochem. Soc. 148 (2001) A30–A37.
[16] M. Onoda, K. Kanbe, J. Phys. Condens. Matter 13 (2001) 6675–6685.
[17] N.D. Leifer, A. Colon, K. Martocci, S.G. Greenbaum, F.M. Alamgir, T.B. Reddy, N.R. Gleason, R.A. Leising, E.S. Takeuchi, J. Electrochem. Soc. 154 (2007) A500–A506.
[18] F. Sauvage, V. Bodenez, H. Vezin, M. Morcrette, J.-M. Tarascon, J. Power Sources 195 (2010) 1195–1201.
[19] M. Grisolia, P. Rozier, M. Benoit, Phys. Rev. B 83 (2011), 165111 (12 pages).
[20] J. Giraudet, M. Dubois, A. Hamwi, W.E.E. Stone, P. Pirotte, F. Masin, J. Phys. Chem. B 109 (2005) 175–181.
[21] J. Giraudet, M. Dubois, K. Guerin, C. Delabarre, A. Hamwi, F. Masin, J. Phys. Chem. B 111 (2007) 14143–14151.
[22] N.D. Leifer, V.S. Johnson, R. Ben-Ari, H. Gan, J.M. Lehnes, R. Guo, W. Lu, B.C. Muffoletto, T. Reddy, P.E. Stallworth, S.G. Greenbaum, J. Electrochem. Soc. 157 (2010) A148–A154.
[23] S. DeSilva, R. Vazquez, P.E. Stallworth, T.B. Reddy, J.M. Lehnes, R. Guo, H. Gan, B.C. Muffoletto, S.G. Greenbaum, J. Power Sources 196 (2011) 5659–5666.
[24] Y. Ahmad, M. Dubois, K. Guerin, A. Hamwi, Z. Fawal, A.P. Kharitonov, A.V. Generalov, A.Y. Klyushin, K.A. Simonov, N.A. Vinogradov, I.A. Zhdanov, A.B. Preobrajenski, A.S. Vinogradov, J. Phys. Chem. C. 117 (2013) 13564–13572.
[25] A. Vyalikh, L.G. Bulusheva, G.N. Chekhova, D.V. Pinakov, A.V. Okotrub, U. Scheler, J. Phys. Chem. C. 117 (2013) 7940–7948.
[26] B.M. Meyer, N. Leifer, S. Sakamoto, S.G. Greenbaum, C.P. Grey, Electrochem. Solid-State Lett. 8 (2005) A145–A148.